Optimal Fractional-order Sliding Mode Controller Design for a class of Fractional-order Nonlinear Systems using particle swarm optimization Algorithm

Djari Abdelhamid *, **Bouden Toufik** * and **Blas M. Vinagre** **

* *NDT Laboratory, Automatic Department, Jijel University, Ouled-Aissa, Jijel,Algeria (e-mail: hamiddjari@yahoo.fr ; bouden-toufik@yahoo.com).*
** *Department of Electrical, Electronic and Automation Engineering, Industrial Engineering school, University of Extremadura, Spain (e-mail: bvinagre@unex.es)*

Abstract: This paper presents a new strategy of the optimal fractional order sliding mode controller (OFSMC) of fractional order non-linear SIMO (Single Input Multiple output) systems based on a division of the global proposed fractional order sliding surface into fractional order sliding sub-surfaces. The optimality of the proposed approach is ensured by the use of PSO algorithm to calculate the parameters λ_i in sliding sub-surfaces, weighting parameters μ_i in global sliding surface and gain k of sign function in the Attractant control (discontinuous control). Simulation results demonstrated the effectiveness of OFSMC by comparing it with the optimal conventional sliding mode control OSMC (optimal integer order SMC) applied on fractional order model of inverted pendulum where OFSMC gives excellent results of robustness.

Keywords: Fractional calculus, fractional order systems, SIMO systems, SMC, FOSMC, PSO algorithm.

1. INTRODUCTION

Fractional calculus is a topic being more than 300 years old but its application to physics and engineering has recently attracted lots of attention (Oldham and Spanier, 1974; Delavari et al., 2010a). The idea of fractional calculus has been known since the regular calculus, with the first reference probably being associated with Leibniz and L'Hospital in 1695 where half-order derivative was mentioned (Petras, 2011). Fractional calculus can be defined as the generalization of classical calculus to orders of integration and differentiation not necessarily integer. Fractional-order control is the use of fractional calculus in the aforementioned topics, the system being modeled in a classical way or as a fractional one. During the past decades, fractional calculus has gained great interest in several applications (Petras, 2011; Podlubny, 1999; Kilbas et al., 2006; Aghababa, 2013). For instance, fractional derivatives can improve the performances and robustness properties in control design of systems (Oustaloup et al., 1995; Oustaloup et al., 1998; Oustaloup et al., 1999; Hosseinia et al., 2012; Hosseinia et al., 2014 ; Calderón et al., 2006). Due to the fact that the fractional order calculus plays an important role in control design, a PD^{α} sliding surface is proposed in (Vinagre and Calderon, 2006; Delavari et al., 2010b; Zhang and Luo, 2012) for fractional sliding mode controller, and a novel fractional integral terminal sliding mode concepts for the output tracking problem of relative-degree-one systems with uncertainty and disturbance is presented in (Chiu, 2012). Also, authors in (Aghababa, 2012) have proposed a novel fractional-order integral type sliding surface for robust stabilization/synchronization problem of a class of fractional order chaotic systems in the presence of model uncertainties and external disturbances. In the present paper, a proposed fractional order sliding mode approach is designed for fractional-order non-linear SIMO systems. A key point of the proposed approach is the selection of a fractional order sliding surface divided into fractional order sliding sub-surfaces, which gives rise to a continuous control input thereby removing the chattering effect. This paper is organized as follows. The next section 2 briefly reviews some preliminaries on fractional calculus. The overview of sliding manifold design procedure of SMC and FOSMC controllers is presented in section 3. Section 4 introduces the particle swarm optimization (PSO) algorithm which's used to design OSMC and OFSMC controllers. The simulation results are highlighted in section 5. The final section 6 draws some concluding remarks.

2. FRACTIONAL ORDER CALCULUS

Several definitions of fractional operators appear in literature. In the current paper the so called Riemann-Liouville approach is adopted. We will present in the following paragraphs, definitions and some properties of Riemann-Liouville fractional differentiation (Podlubny, 1999; Balochian et al., 2011).

2.1 The Gamma function

The Gamma function, denoted $\Gamma(z)$, is a generalization of the factorial function $n!$, ($\Gamma(n) = (n-1)!$ for $n \in N$). For complex arguments z with positive real part, it is defined as:

$$\Gamma(z) = \int_0^{\infty} t^{(z-1)} e^{-t} dt, \; Re(z) > 0 \tag{1}$$

Propriety 01: The important propriety of Gamma function which will be used in the rest of this paper is (Kilbas et al., 2006): If $-m < Re(z) \leq -m+1$ where m is a positive integer, then:

$$\Gamma(z) = \lim_{n \to \infty} \frac{n^z n!}{z(z+1)...(z+n)} \tag{2}$$

with $\quad (z \neq 0; \; z \neq -1; \; \ldots \; z \neq -n)$

2.2 Definition of Riemann-Liouville

Suppose that $\alpha \in R^{+*}, t \in R^{+*}, n \in N$ and $f(t)$ being a causal function, the Riemann-Liouville fractional derivative of order α is defined as (Petras, 2011):

$$D^{\alpha} f(t) = \begin{cases} \dfrac{1}{\Gamma(n-\alpha)} . \dfrac{d^n}{dt^n} \displaystyle\int_0^t \dfrac{f(\tau)}{(t-\tau)^{\alpha+1-n}} d\tau \\ if \; \alpha \in]n-1, n] \\ \dfrac{d^n}{dt^n} f(t) \qquad if \; \alpha = n \end{cases} \tag{3}$$

For $0 < \alpha < 1$, the Riemann-Liouville fractional integration of order is defined as:

$$I^{\alpha} f(t) = \frac{1}{\Gamma(\alpha)} \int_0^t \frac{f(\tau)}{(t-\tau)^{1-\alpha}} d\tau \tag{4}$$

we note that $I^{\alpha} = D^{-\alpha}$ and $D^{\alpha} f(t) = \frac{d^{\alpha}}{dt^{\alpha}} f(t) = f^{(\alpha)}$

2.3 Properties

If $n-1 < \alpha < n$, $(n, m) \in N^2$, $f(t)$ and $g(t)$ are causal functions, then (Li and Deng, 2007):

Propriety 02: $I^{\alpha} D^{\alpha} f(t) = f(t)$ with all initial conditions are nulls.

Propriety 03: $D^{\alpha}(D^{\beta} f(t)) = D^{\beta}(D^{\alpha} f(t)) = D^{\alpha+\beta} f(t)$ with all initial conditions are nulls and $m-1 < \beta < m$.

Propriety 04: $I^{\alpha}(I^{\beta} f(t)) = I^{\beta}(I^{\alpha} f(t)) = I^{\alpha+\beta} f(t)$ with $\beta \in R^{+*}$.

Propriety 05: $D^{\alpha}(\lambda.f(t) + \gamma.g(t)) = \lambda.D^{\alpha} f(t) + \gamma.D^{\alpha} g(t)$.

Propriety 06: $D^{\alpha} c = \frac{c t^{-\alpha}}{\Gamma(1-\alpha)}$ with c is a constant.

3. DESIGNING A FRACTIONAL-ORDER SLIDING MODE CONTROL FOR FRACTIONAL NONLINEAR SYSTEMS

In the conventional sliding mode control (integer SMC), an arbitrary linear manifold is considered as a sliding surface and a control law is planned in such a way that the system state trajectories reach this manifold. In addition, nowadays the sliding mode control is applied for governing the fractional-order systems (Majidabad, 2015; Djari et al., 2014).

3.1 Problem Formulation

We consider a fractional order nonlinear SIMO system given by:

$$\begin{cases} x_1^{(\alpha)} = x_2(t) \\ x_2^{(\alpha)} = f_1(x) + g_1(x).u(t) \\ x_3^{(\alpha)} = x_4(t) \\ x_4^{(\alpha)} = f_2(x) + g_2(x).u(t) \\ \vdots \\ x_{2i-1}^{(\alpha)} = x_{2i}(t) \\ x_{2i}^{(\alpha)} = f_i(x) + g_i(x).u(t) \\ \vdots \\ x_{2n-1}^{(\alpha)} = x_{2n}(t) \\ x_{2n}^{(\alpha)} = f_n(x) + g_n(x).u(t) \end{cases} \tag{5}$$

where:

- $\frac{1}{2} < \alpha < 1$ is a derivative order;
- state vector $x(t)$ is given by: $x(t) = [x_1, x_2, x_3, ..., x_{2n}]^T$;
- $f_i(t)$ and $g_i(t)$, $i = 1, 2, 3, ...n$; are smooth scalar functions with $g_i(t) \neq 0$;
- $u(t)$ is the control signal.

We can easily see that the system (5) contains n subsystems as follows:

$$\begin{cases} x_{2i-1}^{(\alpha)} = x_{2i}(t) \\ x_{2i}^{(\alpha)} = f_i(x) + g_i(x).u(t) \end{cases} \tag{6}$$

We propose in what follows a strategy of fractional order sliding mode control based on the proposal of a fractional order sliding surface as a combination of fractional order sliding subsurfaces. Each subsurface matches the subsystem (6). This approach will be compared with integer SMC where the sliding surface is also a combination of integer order sliding subsurfaces.

3.2 Integer Sliding Mode Control

Let us consider the following proposal integer order surfaces:

$$\begin{cases} s_1 = \dot{e}_1 + \lambda_1.e_1 \\ s_2 = \dot{e}_3 + \lambda_2.e_3 \\ s_3 = \dot{e}_5 + \lambda_3.e_5 \\ \vdots \\ s_i = \dot{e}_{2i-1} + \lambda_i.e_{2i-1} \\ \vdots \\ s_n = \dot{e}_{2n-1} + \lambda_n.e_{2n-1} \end{cases} \tag{7}$$

where:

- $\lambda_i > 0$, $i = 1, 2, 3, ...n$;
- $e_{2i-1} = x_{2i-1} - x_{d2i-1}$ is a component of tracking error;
- x_{d2i-1} is a given component of a reference trajectory

The subsurface s_i corresponds the subsystem (6).
To design a control $u(t)$ signal for the system (5), we will define the following integer order sliding function:

$$S = \sum_{i=1}^{n}(\mu_i.s_i) = \sum_{i=1}^{n}(\mu_i.(\dot{e}_{2i-1} + \lambda_i.e_{2i-1})); \quad \mu_i > 0 \quad (8)$$

On the sliding surface $S = 0$, the state variables of the sub-systems have reached the sliding sub-surfaces $s_i = 0$ and also tend towards the origin of the phase plane of the global system. In this equilibrium point, the control signal should force the trajectories of states to remain around this point if $t \longrightarrow \infty$.

The μ_i coefficients are selected by the designer according to the importance of an output to another output or we let the automatic optimization of its values using PSO algorithm via a predefined objective function (cost function).

Taking the time derivative of (8), one can obtain:

$$\dot{S} = \sum_{i=1}^{n}(\mu_i.(e^{(2)}_{2i-1} + \lambda_i.\dot{e}_{2i-1})) \quad (9)$$

Forcing $\dot{S} = 0$, (9) yields:

$$\dot{S} = \sum_{i=1}^{n}(\mu_i.(e^{(2)}_{2i-1} + \lambda_i.\dot{e}_{2i-1})) = 0 \quad (10)$$

Since $\frac{1}{2} < \alpha < 1$ and all initial conditions are nulls; we can rewrite (10) as follows:

$$\sum_{i=1}^{n}(\mu_i.(D^{2(1-\alpha)}(e^{(2\alpha)}_{2i-1}) + \lambda_i.\dot{e}_{2i-1})) = 0 \quad (11)$$

$$\Longrightarrow \sum_{i=1}^{n}(\mu_i.(D^{2(1-\alpha)}(x^{(2\alpha)}_{2i-1} - x^{(2\alpha)}_{d2i-1}) + \lambda_i.\dot{e}_{2i-1})) = 0 \quad (12)$$

From (5), we have:

$$x^{(\alpha)}_{2i-1} = x_{2i} \Longrightarrow \; x^{(2\alpha)}_{2i-1} = x^{(\alpha)}_{2i}$$
$$and \;\; x^{(\alpha)}_{2i} = f_i(x) + g_i(x).u(t) \quad (13)$$

Equation (12) yields:

$$\sum_{i=1}^{n}(\mu_i.(D^{2(1-\alpha)}(f_i(x) + g_i(x).u(t) - x^{(2\alpha)}_{d2i-1}) + \lambda_i.\dot{e}_{2i-1})) = 0 \quad (14)$$

It will be:

$$D^{2(1-\alpha)}\sum_{i=1}^{n}(\mu_i.g_i(x).u(t)) = -\sum_{i=1}^{n}(\mu_i.(D^{2(1-\alpha)}(f_i(x) - x^{(2\alpha)}_{d2i-1}) + \lambda_i.\dot{e}_{2i-1})) \quad (15)$$

Integrating both sides by order $2(1-\alpha)$ (or derivate by order $2(\alpha-1)$), yields:

$$\sum_{i=1}^{n}(\mu_i.g_i(x)).u(t) = -\sum_{i=1}^{n}(\mu_i.(f_i(x) - x^{(2\alpha)}_{d2i-1} + \lambda_i.e^{(2\alpha-1)}_{2i-1})) \quad (16)$$

Notice that the last equality is a consequence of all initial conditions being zeros; otherwise it would not be necessarily true (Li and Deng, 2007). Equation (16) yields:

$$u(t).\sum_{i=1}^{n}(\mu_i.g_i(x)) = \sum_{i=1}^{n}(\mu_i.(-f_i(x) + x^{(2\alpha)}_{d2i-1} - \lambda_i.e^{(2\alpha-1)}_{2i-1})) \quad (17)$$

The continuous control signal $u_c(t)$ is given by:

$$u_c(t) = \frac{\sum_{i=1}^{n}(\mu_i.(-f_i(x) + x^{(2\alpha)}_{d2i-1} - \lambda_i.e^{(2\alpha-1)}_{2i-1}))}{\sum_{i=1}^{n}(\mu_i.g_i(x))}$$
$$with \;\sum_{i=1}^{n}(\mu_i.g_i(x)) \neq 0 \quad (18)$$

The global control signal designed is equal to the continuous control $u_c(t)$ plus the attractant (discontinuous) control $u_n(t)$: $u(t) = u_c(t) + u_n(t)$ with $u_n(t) = \frac{-k.sgn(S)}{\sum_{i=1}^{n}(\mu_i.g_i(x))}$; so:

$$u(t) = \frac{\sum_{i=1}^{n}(\mu_i.(-f_i(x) + x^{(2\alpha)}_{d2i-1} - \lambda_i.e^{(2\alpha-1)}_{2i-1})) - k.sgn(S)}{\sum_{i=1}^{n}(\mu_i.g_i(x))} \quad (19)$$

- Verification of the reachability condition

Let us consider the Lyapunov candidate function $V = \frac{1}{2}S^2$ which used to verify the reachability condition $\dot{V} = S.\dot{S} \leq 0$ of proposed control. We obtain (20) using expression (14):

$$\dot{S} = \sum_{i=1}^{n}(\mu_i.(D^{2(1-\alpha)}(f_i(x) + g_i(x).u(t) - x^{(2\alpha)}_{d2i-1}) + \lambda_i.\dot{e}_{2i-1})) \quad (20)$$

$$\Longrightarrow \dot{S} = \sum_{i=1}^{n}(D^{2(1-\alpha)}\mu_i.g_i(x).u(t)) + \sum_{i=1}^{n}(\mu_i.(D^{2(1-\alpha)}(f_i(x) - x_{d_{2i-1}}^{(2\alpha)}) + \lambda_i.\dot{e}_{2i-1})) \quad (21)$$

$$\Longrightarrow \dot{S} = D^{2(1-\alpha)}\sum_{i=1}^{n}(\mu_i.g_i(x).u(t)) + \sum_{i=1}^{n} D^{2(1-\alpha)}(\mu_i.((f_i(x) - x_{d_{2i-1}}^{(2\alpha)}) + \lambda_i.e_{2i-1}^{(2\alpha-1)})) \quad (22)$$

Substituting (18) into (22), we obtain:

$$\dot{S} = D^{2(1-\alpha)}\left[\sum_{i=1}^{n}(\mu_i.(-f_i(x) + x_{d_{2i-1}}^{(2\alpha)} - \lambda_i.e_{2i-1}^{(2\alpha-1)})) - k.sgn(S)\right] + D^{2(1-\alpha)}\sum_{i=1}^{n}(\mu_i.(f_i(x) - x_{d_{2i-1}}^{(2\alpha)} + \lambda_i.e_{2i-1}^{(2\alpha-1)})) \quad (23)$$

$$\Longrightarrow \dot{S} = D^{2(1-\alpha)}\left[-k.sgn(S)\right] \quad (24)$$

$$\Longrightarrow \frac{-\dot{S}}{k} = D^{2(1-\alpha)}sgn(S) \quad (25)$$

$$\Longrightarrow sgn\left(\frac{-\dot{S}}{k}\right) = sgn\left(D^{2(1-\alpha)}sgn(S)\right) \quad (26)$$

We can easily demonstrate that:

$$sgn\left(D^{2(1-\alpha)}sgn(S)\right) = sgn(S) \quad (propriety\ 07) \quad (27)$$

Propriety 07: If $S(t)$ is a continuous function and $\frac{1}{2} < \alpha < 1$ then: $sgn\left(D^{2(1-\alpha)}sgn(S)\right) = sgn(S)$

Proof. if $c = constant$ and $\frac{1}{2} < \alpha < 1$ then $D^{\alpha}c = \frac{ct^{-\alpha}}{\Gamma(1-\alpha)}$ (*subsection 2.3; propriety 06*) with:

$$D^{2(1-\alpha)}c = \frac{ct^{2(\alpha-1)}}{\Gamma(2\alpha-1)} \quad (28)$$

and

$$\Gamma(2\alpha-1) = \lim_{n\to\infty}\frac{n^{2\alpha-1}n!}{(2\alpha-1)(2\alpha)...(2\alpha+n)} \quad (29)$$

(*subsection* 2.1; *propriety*01)

We note that $\Gamma(2\alpha-1) > 0$ ($\forall\ n > 0$ and $\frac{1}{2} < \alpha < 1$) and ($t^{2(\alpha-1)} > 0\ \forall\ t > 0$), so:

$$sgn(S) = \begin{cases} 1 & if\ S > 0 \\ -1 & if\ S < 0 \\ 0 & if\ S = 0 \end{cases} \quad (30)$$

$$\Rightarrow D^{2(1-\alpha)}sgn(S) = \begin{cases} D^{2(1-\alpha)}(1) & if\ S > 0 \\ D^{2(1-\alpha)}(-1) & if\ S < 0 \\ D^{2(1-\alpha)}(0) & if\ S = 0 \end{cases} \quad (31)$$

$$\Rightarrow D^{2(1-\alpha)}sgn(S) = \begin{cases} \frac{t^{2(\alpha-1)}}{\Gamma(2\alpha-1)} & if\ S > 0 \\ \frac{-t^{2(\alpha-1)}}{\Gamma(2\alpha-1)} & if\ S < 0 \\ 0 & if\ S = 0 \end{cases} \quad (32)$$

$$\Rightarrow sgn(D^{2(1-\alpha)}sgn(S)) = \begin{cases} sgn(\frac{t^{2(\alpha-1)}}{\Gamma(2\alpha-1)}) & if\ S > 0 \\ sgn(\frac{-t^{2(\alpha-1)}}{\Gamma(2\alpha-1)}) & if\ S < 0 \\ sgn(0) & if\ S = 0 \end{cases} \quad (33)$$

$$\Rightarrow sgn(D^{2(1-\alpha)}sgn(S)) = \begin{cases} 1 & if\ S > 0 \\ -1 & if\ S < 0 \\ 0 & if\ S = 0 \end{cases} \quad (34)$$

$$\Rightarrow sgn(D^{2(1-\alpha)}sgn(S)) = Sgn(S) \quad (35)$$

Equation (26) yields:

$$\Longrightarrow sgn\left(\frac{-\dot{S}}{k}\right) = sgn(S) \quad (36)$$

with:

$$sgn(S) = \begin{cases} 1 & if\ S > 0 \\ -1 & if\ S < 0 \\ 0 & if\ S = 0 \end{cases} \quad (37)$$

and :

$$sgn(\frac{-\dot{S}}{k}) = \begin{cases} 1 & if\ (\frac{-\dot{S}}{k}) > 0 \\ -1 & if\ (\frac{-\dot{S}}{k}) < 0 \\ 0 & if\ (\frac{-\dot{S}}{k}) = 0 \end{cases} \quad (38)$$

We have three cases:

- case 01:

$$sgn(\frac{-\dot{S}}{k}) = sgn(S) = 1\ \Rightarrow (\frac{-\dot{S}}{k}) > 0\ and\ S > 0 \Rightarrow S.(\frac{-\dot{S}}{k}) > 0\ \Rightarrow S.\dot{S} < 0;\ (k > 0). \quad (39)$$

- case 02:

$$sgn(\frac{-\dot{S}}{k}) = sgn(S) = -1\ \Rightarrow (\frac{-\dot{S}}{k}) < 0\ and\ S < 0 \Rightarrow S.(\frac{-\dot{S}}{k}) > 0\ \Rightarrow S.\dot{S} < 0;\ (k > 0). \quad (40)$$

- case 03:

$$sgn(\frac{-\dot{S}}{k}) = sgn(S) = 0\ \Rightarrow (\frac{-\dot{S}}{k}) = 0\ and\ S = 0 \Rightarrow S.(\frac{-\dot{S}}{k}) = 0\ \Rightarrow S.\dot{S} = 0;\ (k > 0). \quad (41)$$

So, all cases prove that the proposed form of the control signal causes ($\dot{V} = S.\dot{S} \leq 0$), which verifies the reaching condition.

3.3 Fractional-order sliding mode control

Let us consider the following proposal fractional order surfaces:

$$\begin{cases} s_1 = e_1^{(\alpha)} + \lambda_1.e_1 \\ s_2 = e_3^{(\alpha)} + \lambda_2.e_3 \\ s_3 = e_5^{(\alpha)} + \lambda_3.e_5 \\ \vdots \\ s_i = e_{2i-1}^{(\alpha)} + \lambda_i.e_{2i-1} \\ \vdots \\ s_n = e_{2n-1}^{(\alpha)} + \lambda_n.e_{2n-1} \end{cases} \quad (42)$$

where:

- $\lambda_i > 0$ with $i = 1, 2, 3, ...n;$;
- $e_{2i-1} = x_{2i-1} - x_{d2i-1}$ is a component of tracking error;
- x_{d2i-1} is a component of a reference trajectory

The subsurface s_i corresponds to the subsystem (6).

As we noted in section (4.1), we will define the following fractional order sliding function to design a control $u(t)$ signal for the system (5):

$$S = \sum_{i=1}^{n}(\mu_i.s_i) = \sum_{i=1}^{n}(\mu_i.(e_{2i-1}^{(\alpha)} + \lambda_i.e_{2i-1})); \quad \mu_i > 0 \quad (43)$$

Taking the time derivative of (43), one can obtain:

$$\dot{S} = \sum_{i=1}^{n}(\mu_i.(e_{2i-1}^{(1+\alpha)} + \lambda_i.\dot{e}_{2i-1})) \quad (44)$$

Forcing $\dot{S} = 0$, we have:

$$\dot{S} = \sum_{i=1}^{n}(\mu_i.(e_{2i-1}^{(1+\alpha)} + \lambda_i.\dot{e}_{2i-1})) = 0 \quad (45)$$

Since $\frac{1}{2} < \alpha < 1$ and all initial conditions are nulls; we can rewrite (45) as follows:

$$\sum_{i=1}^{n}(\mu_i.(D^{1-\alpha}(e_{2i-1}^{(2\alpha)}) + \lambda_i.e_{2i-1}^{(\alpha)})) = 0 \quad (46)$$

$$\Longrightarrow \sum_{i=1}^{n}(\mu_i.(D^{1-\alpha}(x_{2i-1}^{(2\alpha)} - x_{d2i-1}^{(2\alpha)}) + \lambda_i.e_{2i-1}^{(\alpha)})) = 0 \quad (47)$$

From (5), we have:

$$\begin{array}{c} x_{2i-1}^{(\alpha)} = x_{2i} \Longrightarrow \; x_{2i-1}^{(2\alpha)} = x_{2i}^{(\alpha)} \\ and \; x_{2i}^{(\alpha)} = f_i(x) + g_i(x).u(t) \end{array} \quad (48)$$

Equation (47) yields:

$$\sum_{i=1}^{n}(\mu_i.(D^{1-\alpha}(f_i(x) + g_i(x).u(t) - x_{d2i-1}^{(2\alpha)}) + \lambda_i.e_{2i-1}^{(\alpha)})) = 0 \quad (49)$$

It will be:

$$\begin{array}{c} D^{1-\alpha}\sum_{i=1}^{n}(\mu_i.g_i(x).u(t)) = \\ -\sum_{i=1}^{n}(\mu_i.(D^{1-\alpha}(f_i(x) - x_{d2i-1}^{(2\alpha)}) + \lambda_i.e_{2i-1}^{(\alpha)})) \end{array} \quad (50)$$

Integrating both sides by order $(1-\alpha)$ (or derivate by order $(\alpha - 1)$), yields:

$$\begin{array}{c} \sum_{i=1}^{n}(\mu_i.g_i(x)).u(t) = \\ -\sum_{i=1}^{n}(\mu_i.(f_i(x) - x_{d2i-1}^{(2\alpha)} + \lambda_i.e_{2i-1}^{(\alpha)})) \end{array} \quad (51)$$

Notice that the last equality is a consequence of all initial conditions being zeros; otherwise it would not be necessarily true (Li and Deng, 2007). Equation (51) yields:

$$\begin{array}{c} u(t).\sum_{i=1}^{n}(\mu_i.g_i(x)) = \\ \sum_{i=1}^{n}(\mu_i.(-f_i(x) + x_{d2i-1}^{(2\alpha)} - \lambda_i.e_{2i-1}^{(\alpha)})) \end{array} \quad (52)$$

The continuous control signal $u_c(t)$ is given by:

$$\begin{array}{c} u_c(t) = \frac{\sum_{i=1}^{n}(\mu_i.(-f_i(x) + x_{d2i-1}^{(2\alpha)} - \lambda_i.e_{2i-1}^{(\alpha)}))}{\sum_{i=1}^{n}(\mu_i.g_i(x))} \\ with \; \sum_{i=1}^{n}(\mu_i.g_i(x)) \neq 0 \end{array} \quad (53)$$

The global control signal designed is equal to the continuous control $u_c(t)$ plus the attractant (discontinuous) control $u_n(t)$: $u(t) = u_c(t) + u_n(t)$ with $u_n(t) = \frac{-k.sgn(S)}{\sum_{i=1}^{n}(\mu_i.g_i(x))}$; so:

$$\begin{array}{c} u(t) = \\ \frac{\sum_{i=1}^{n}(\mu_i.(-f_i(x) + x_{d2i-1}^{(2\alpha)} - \lambda_i.e_{2i-1}^{(\alpha)})) - k.sgn(S)}{\sum_{i=1}^{n}(\mu_i.g_i(x))} \end{array} \quad (54)$$

- Verification of the reachability condition

Taking the same Lyapunov candidate function $V = \frac{1}{2}S^2$ which used above to verify the reachability condition $\dot{V} = S.\dot{S} \leq 0$. From equation (49), one can obtain:

$$\begin{array}{c} \dot{S} = D^{1-\alpha}\sum_{i=1}^{n}(\mu_i.g_i(x).u(t)) + \\ \sum_{i=1}^{n} D^{1-\alpha}(\mu_i.((f_i(x) - x_{d2i-1}^{(2\alpha)}) + \lambda_i.e_{2i-1}^{(2\alpha-1)})) \end{array} \quad (55)$$

$$\begin{array}{c} \Rightarrow \qquad \dot{S} = \\ D^{1-\alpha}\left[\sum_{i=1}^{n}(\mu_i.(-f_i(x) + x_{d2i-1}^{(2\alpha)} - \lambda_i.e_{2i-1}^{(\alpha)})) - k.sgn(S)\right] \end{array} \quad (56)$$

$$+D^{1-\alpha}\sum_{i=1}^{n}(\mu_i.(f_i(x) - x_{d2i-1}^{(2\alpha)} + \lambda_i.e_{2i-1}^{(\alpha)}))$$

$$\Longrightarrow \dot{S} = D^{1-\alpha}\left[-k.sgn(S)\right] \quad (57)$$

$$\Longrightarrow \frac{-\dot{S}}{k} = D^{1-\alpha} sgn(S) \tag{58}$$

$$\Longrightarrow sgn\left(\frac{-\dot{S}}{k}\right) = sgn\left(D^{1-\alpha} sgn(S)\right) \tag{59}$$

We demonstrate, $sgn\left(D^{1-\alpha} sgn(S)\right) = sgn(S)$ using the same stages of propriety 07. Equation (59) yields:

$$sgn\left(\frac{-\dot{S}}{k}\right) = sgn(S) \tag{60}$$

We have the same cases studied in above paragraph (with integer form of SMC). So, the proposed form of the FSMC control signal causes $\dot{V} = S.\dot{S} \leq 0$.

The representation of the proposed OFSMC control systems is described in the flowing figure (fig.1).

Remark 01: If there is a singularity in the expression of the control signal ($\sum_{i=1}^{n}(\mu_i.g_i(x)) = 0$)*, we can add a very small value tends to zero* ($\epsilon \to 0$) *to this term for avoid the division by zero.*

4. PARTICLE SWARM OPTIMIZATION ALGORITHM

Particle swarm optimization (PSO) is an evolutionary computation technique developed by Kennedy and Eberhart in 1995 (Eberhart, and Kennedy, 1995). The inspiration underlying the development of this algorithm was the social behaviour of animals, such as the flocking of birds and the schooling of fish, and the swarm theory. It has been proven to be efficient in solving optimization problem especially for nonlinearity and non differentiability, multiple optimum, and high dimensionality (Chang and Shih, 2010; Chiou and Liu, 2009). In PSO algorithm, the velocity of each particle is modified iteratively by its individual best position (p_{best}), and the best position found by particles in its neighborhood, named global best position, (g_{best}). As a result, each particle searches around a region defined by its individual best position (p_{best}) and the global best position (g_{best}) from its neighborhood. Henceforth we use (V_i) to denote the velocity of the i^{th} particle in the swarm, p_i denote its position. At each step (iteration) n, by using the individual best position, p_{best}, and global best position, g_{best}, the velocity and position of each particle are updated by the following tow equations:

$$\begin{aligned} V_i(n) = \omega.\left[V_i(n-1) + c_1.r_1.(p_{best_i} - p_i(n-1))\right] \\ +\omega.\left[c_2.r_2.(g_{best} - p_i(n-1))\right] \end{aligned} \tag{61}$$

$$p_i(n) = p_i(n-1) + V_i(n) \tag{62}$$

Where r_1 and r_2 are random numbers between 0 and 1; c_1 and c_2 are positive constant learning rates; ω is called the constriction factor (Clerc, 1999) and is defined by (63):

$$\omega = \frac{2}{\left|2 - c - \sqrt{c^2 - 4c}\right|} \;\; ; \; c = c_1 + c_2. \tag{63}$$

In each step or iteration n the position is confined within the range of $[p_{min}, p_{max}]$. If the position violates these limits, it is forced to its proper values (Chang and Shih, 2010; Shi and Eberhart, 1999):

$$p_i = \begin{cases} p_{min} \;\; if & p_i < p_{min} \\ p_i \;\; if & p_{min} < p_i < p_{max} \\ p_{max} \;\; if & p_i > p_{max} \end{cases} \tag{64}$$

Changing position by this way enables the i^{th} particle to search around its local best position, p_{best}, and global best position,g_{best}.
The following shows the design step for implementing the PSO algorithm (Chang and Shih, 2010):

- **Step 1.** Initialize particles with random position and velocity on dimension in the problem space;
- **Step 2.** If a prescribed number of iterations (generations) is achieved, and then stop the algorithm;
- **Step 3.** For each particle, evaluate the desired optimization fitness function, and record each particle's best previous position (p_{best}), and global best position (g_{best});
- **Step 4.** Change the velocity and position according to equations (61) and (62) respectively, for each particle;
- **Step 5.** Check each particle's position using (64);
- **Step 6.** Go back to Step 2.

Remark 02: We use the abbreviations OSMC and OFSMC when using the PSO algorithm optimization of the parameters of designed controllers SMC and FSMC respectively.

To converge toward the optimal solution, the PSO algorithm must be guided by the cost function (objective function). Hence, it should be properly defined before the PSO algorithm is executed. In the present study, the used cost function (F_1) is defined by the following formula:

$$F_1 = \sum_{k=1}^{N}\left[\sum_{i=1}^{n}\left(|e_{2i-1}(k)|^2\right) + |u(k)|^2\right] \tag{65}$$

Where $e_{2i-1}(k)$ is the trajectory error of k^{th} sample, $u(k)$ is the control signal of k^{th} sample, n is the number of subsystems in the global system to be controlled (Problem Formulation) and N is the number of samples.

5. SIMULATION RESULTS

In this section, we will give an illustrative example to show the applicability and efficiency of the proposed controllers (OSMC and OFSMC). The simulation is carried out using the "'Matlab/Simulink"' tools with 0.01 sample time. The population size of PSO algorithm is set to 15 particles; the parameters c_1 and c_2 are set to 2.05 respectively and the maximum number of iteration n is set to 15 iterations. Let $P = [k\ \lambda_1\ \lambda_2\ \mu_1\ \mu_2]^T$ the vector of selective parameters of OSMC and OFSMC, the regions of the decision variables are mentioned as follows: $0.1 < k < 20$; $0.1 < \lambda_1 < 3$; $0.1 < \lambda_2 < 6$; $0.1 < \mu_1 < 20$; $0.1 < \mu_2 < 6$

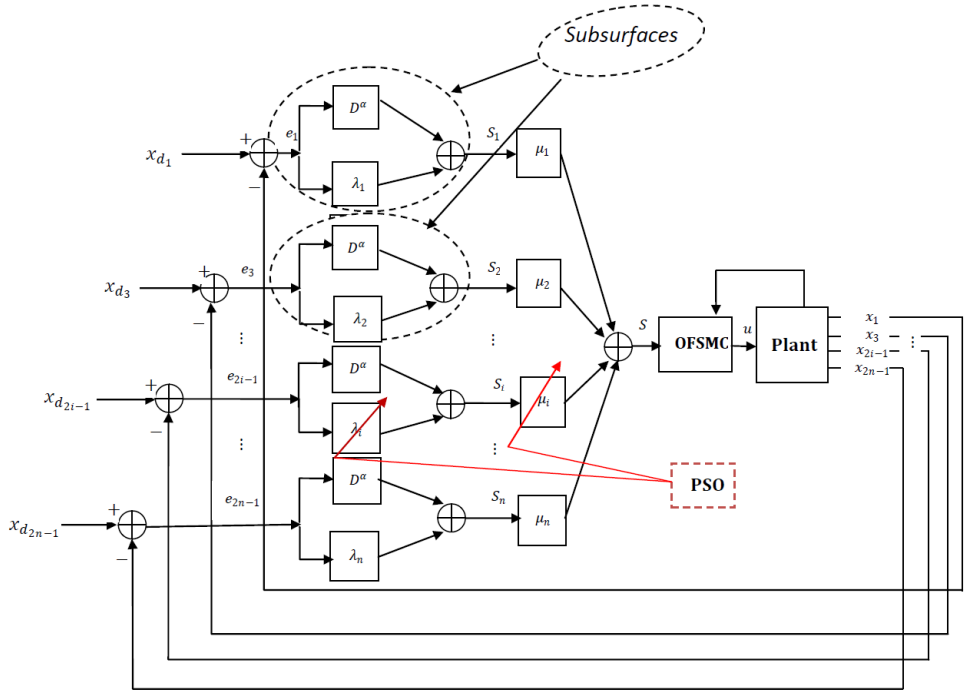

Fig. 1. Block diagram of the proposed OFSMC control system.

In this illustrative example, we present simulation results showing the state time responses for tracking both references. Let us consider the dynamic of inverted pendulum which given by (66), (Ji-Hyuk et al., 2009; Prasad et al., 2012; Nour et al., 2007):

We put: $y_1 = x_1$; $y_2 = x_3$; $[x_1\ x_2\ x_3\ x_4]^T = [x\ \dot{x}\ \theta\ \dot{\theta}]^T$

$$\begin{cases} \dot{x}_1 = x_2 \\ \dot{x}_2 = \dfrac{-m^2l^2g.cos(x_3)sin(x_3) + mld.cos(x_3)x_4}{hN - m^2l^2.cos^2(x_3)} \\ + \dfrac{mlN.sin(x_3)x_4^2 - bN.x_2}{hN - m^2l^2.cos^2(x_3)} + \dfrac{N}{hN - m^2l^2.cos^2(x_3)}.F \\ \dot{x}_3 = x_4 \\ \dot{x}_4 = \dfrac{mgl}{N}.sin(x_3) - \dfrac{d}{N}.x_4 \\ + \dfrac{cos(x_3)\left[m^3l^3g.cos(x_3)sin(x_3) - m^2l^2d.cos(x_3)x_4\right]}{N\left(hN - m^2l^2.cos^2(x_3)\right)} \\ + \dfrac{cos(x_3)\left[-m^2l^2N.sin(x_3)x_4^2 + mlbN.x_2\right]}{N\left(hN - m^2l^2.cos^2(x_3)\right)} \\ - \dfrac{ml.cos(x_3)}{hN - m^2l^2.cos^2(x_3)}.F \end{cases} \quad (66)$$

Since the control force F, in terms of the motor voltage V_c, can be expressed as (Prasad et al., 2012):

$$F = \frac{rk_mV_c - k_mk_bx_2}{R_ar^2} \quad (67)$$

where x_2 is the velocity of the cart, K_m is the motor torque constant, K_b is the gearbox ratio, R is the motor armature resistance and r is the radius of driving gear.

When the control variable of the model is the control voltage V_c, it is enough to substitute the force F by its expression depending on the voltage control V_c, we obtain:

$$\begin{cases} \dot{x}_1 = x_2 \\ \dot{x}_2 = \dfrac{-m^2l^2g.cos(x_3)sin(x_3) + mld.cos(x_3)x_4}{hN - m^2l^2.cos^2(x_3)} \\ + \dfrac{mlN.sin(x_3)x_4^2 - bN.x_2}{hN - m^2l^2.cos^2(x_3)} \\ - \dfrac{Nk_mk_bx_2}{R_ar^2\left(hN - m^2l^2.cos^2(x_3)\right)} \\ + \dfrac{Nk_m}{R_ar\left(hN - m^2l^2.cos^2(x_3)\right)}.V_c \\ \dot{x}_3 = x_4 \\ \dot{x}_4 = \dfrac{mgl}{N}.sin(x_3) - \dfrac{d}{N}.x_4 \\ + \dfrac{cos(x_3)\left[m^3l^3g.cos(x_3)sin(x_3) - m^2l^2d.cos(x_3)x_4\right]}{N\left(hN - m^2l^2.cos^2(x_3)\right)} \\ + \dfrac{cos(x_3)\left[-m^2l^2N.sin(x_3)x_4^2 + mlbN.x_2\right]}{N\left(hN - m^2l^2.cos^2(x_3)\right)} \\ - \dfrac{k_mk_bml.cos(x_3)x_2}{R_ar^2\left(hN - m^2l^2.cos^2(x_3)\right)} \\ + \dfrac{k_mml.cos(x_3)}{R_ar\left(hN - m^2l^2.cos^2(x_3)\right)}.V_c \end{cases} \quad (68)$$

In what follows, we propose a fractional form of the this model state as follows with: $\frac{1}{2} < \alpha < 1$ and $u = V_c$;

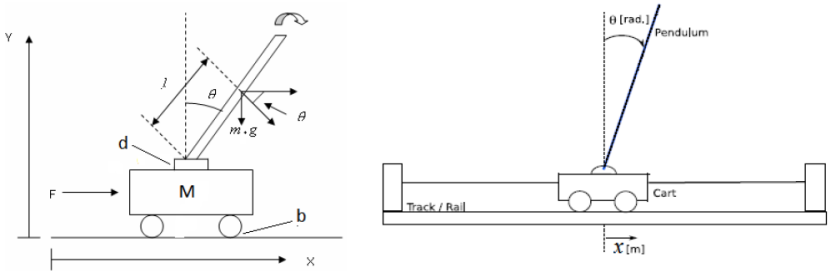

Fig. 2. Inverted pendulum system.

$$\begin{cases} x_1^{(\alpha)} = x_2(t) \\ x_2^{(\alpha)} = f_1(x) + g_1(x).u(t) \\ x_3^{(\alpha)} = x_4(t) \\ x_4^{(\alpha)} = f_2(x) + g_2(x).u(t) \\ y = [x_1, x_3]^T \end{cases} \tag{69}$$

with:

$$\begin{cases} f_1 = \dfrac{-m^2l^2g.cos(x_3)sin(x_3) + mld.cos(x_3)x_4}{hN - m^2l^2.cos^2(x_3)} \\ \quad + \dfrac{mlN.sin(x_3)x_4^2 - bN.x_2}{hN - m^2l^2.cos^2(x_3)} \\ \quad - \dfrac{Nk_mk_bx_2}{R_ar^2\,(hN - m^2l^2.cos^2(x_3))} \\ g_1 = \dfrac{Nk_m}{R_ar\,(hN - m^2l^2.cos^2(x_3))} \\ f_2 = \dfrac{mgl}{N}.sin(x_3) - \dfrac{d}{N}.x_4 \\ + \dfrac{cos(x_3)\left[m^3l^3g.cos(x_3)sin(x_3) - m^2l^2d.cos(x_3)x_4\right]}{N\,(hN - m^2l^2.cos^2(x_3))} \\ + \dfrac{cos(x_3)\left[-m^2l^2N.sin(x_3)x_4^2 + mlbN.x_2\right]}{N\,(hN - m^2l^2.cos^2(x_3))} \\ - \dfrac{k_mk_bml.cos(x_3)x_2}{R_ar^2\,(hN - m^2l^2.cos^2(x_3))} \\ g_2 = \dfrac{k_mml.cos(x_3)}{R_ar\,(hN - m^2l^2.cos^2(x_3))} \end{cases} \tag{70}$$

We propose this fractional order model with $\alpha = 0.95$ just to show the applicability of the proposed controllers and this value of α is approximately equal to 1 which means the same model integer order model of inverted pendulum.

The numerical simulations are done with the following system parameters: $m = 0.2kg$, $b = 5.10^{-5}Nsm^{-1}$, $M = 2.3kg$, $l = 0.3m$, $g = 9.81ms^{-2}$, $R_a = 2.5\Omega$, $k_m = 0.05Nm$, $d = 0.005N.ms.rad^{-1}$, $k_b = 0.05NA^{-1}$, $h = M + m$, $r = 0.0027m$, $J = 1.4.10^{-5}kgm^2$, $N = ml^2 + J$. We also assume that the order of derivatives in the fractional model is $\alpha = 0.95$ and the all initial conditions are nulls ($[\mathrm{x}_1\ x_2\ x_3\ x_4]^T = [0\ 0\ 0\ 0]^T$).

5.1 Designing of optimal sliding mode control

The sliding function $S(t)$ and the control signal $u(t)$ are given by (71) and (73) respectively:

$$\begin{aligned} S &= \sum_{i=1}^{2}\mu_i s_i = \sum_{i=1}^{2}\mu_i(\dot{e}_{2i-1} + \lambda_i e_{2i-1}) \\ &= \mu_1(\dot{e}_1 + \lambda_1 e_1) + \mu_2(\dot{e}_3 + \lambda_2 e_3) \end{aligned} \tag{71}$$

$$u(t) = \frac{\sum_{i=1}^{2}(\mu_i.(-f_i(x) + x_{d2i-1}^{(2\alpha)} - \lambda_i.e_{2i-1}^{(2\alpha-1)}))}{\sum_{i=1}^{2}(\mu_i.g_i(x))} - \frac{k.sgn(S)}{\sum_{i=1}^{2}(\mu_i.g_i(x))} \tag{72}$$

$$\Rightarrow\ u(t) = \frac{\mu_1.(-f_1(x) + x_{d1}^{(2\alpha)} - \lambda_1.e_1^{(2\alpha-1)})}{\mu_1.g_1(x) + \mu_2.g_2(x)} + \frac{\mu_2.(-f_2(x) + x_{d3}^{(2\alpha)} - \lambda_2.e_3^{(2\alpha-1)}) - k.sgn(S)}{\mu_1.g_1(x) + \mu_2.g_2(x)} \tag{73}$$

5.2 Designing of optimal fractional sliding mode control

In this application, the sliding function $S(t)$ and the control signal $u(t)$ are given by (74) and (76) respectively:

$$\begin{aligned} S &= \sum_{i=1}^{2}\mu_i s_i = \sum_{i=1}^{2}\mu_i({e^{(\alpha)}}_{2i-1} + \lambda_i e_{2i-1}) \\ &= \mu_1(e_1^{(\alpha)} + \lambda_1 e_1) + \mu_2(e_3^{(\alpha)} + \lambda_2 e_3) \end{aligned} \tag{74}$$

$$u(t) = \frac{\sum_{i=1}^{2}(\mu_i.(-f_i(x) + x_{d2i-1}^{(2\alpha)} - \lambda_i.e_{2i-1}^{(\alpha)}))}{\sum_{i=1}^{2}(\mu_i.g_i(x))} - \frac{k.sgn(S)}{\sum_{i=1}^{2}(\mu_i.g_i(x))} \tag{75}$$

$$\Rightarrow\ u(t) = \frac{\mu_1.(-f_1(x) + x_{d1}^{(2\alpha)} - \lambda_1.e_1^{(\alpha)})}{\mu_1.g_1(x) + \mu_2.g_2(x)} \frac{+\mu_2.(-f_2(x) + x_{d3}^{(2\alpha)} - \lambda_2.e_3^{(\alpha)}) - k.sgn(S)}{\mu_1.g_1(x) + \mu_2.g_2(x)} \tag{76}$$

We use two cases of references trajectories:

- case 01: In the 1^{st} case, the 1^{st} reference is a periodic orbit $sin(0.2t)$ and the 2^{nd} equal to $-\pi$;
- case 02: In the 2^{nd} case, we use the 1^{st} reference equal to unit ramp signal t and the 2^{nd} equal to $\frac{-\pi}{15}$.

5.3 Simulation results in 1^{st} case and 2^{nd} case

The optimal parameters obtained after optimization of 1^{st} case ($x_{d1} = sin(0.2t)$ and $x_{d3} = -\pi$), 2^{nd} case

($x_{d1} = t$ and $x_{d3} = \frac{-\pi}{15}$) are given in table 1 and table 2 respectevly. The simulation results of 1^{st} case and 2^{nd} case are presented in figures (3-9) and figures (20-27) respectevly.

Table 1. Optimal parameters obtained of OSMC and OFSMC in the 1^{st} case

	k	λ_1	λ_2	μ_1	μ_2
OSMC	12.0000	2.9600	1.0000	10.9459	0.5100
OFSMC	7.1196	0.4268	1.0000	15.0000	0.5100

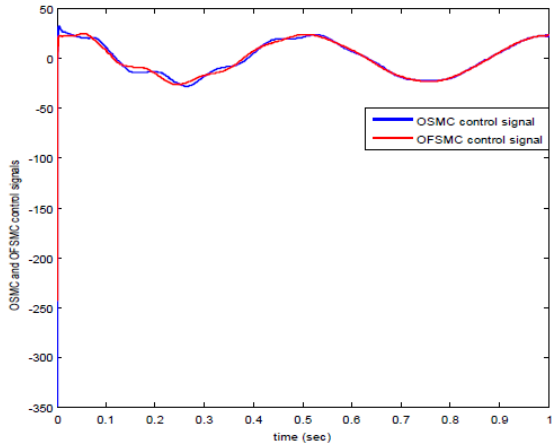

Fig. 3. OSMC and OFSMC Control signals (1^{st} case).

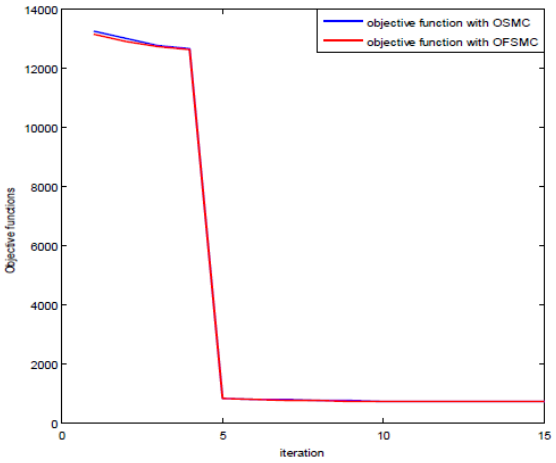

Fig. 4. Objective functions with OSMC and OFSMC (1^{st} case).

Table 2. Optimal parameters obtained of OSMC and OFSMC in the 2^{nd} case

	k	λ_1	λ_2	μ_1	μ_2
OSMC	1.3665	0.9500	5.5000	9.0000	5.0000
OFSMC	2.5324	0.9500	5.5000	9.0000	5.0000

5.4 Discussion and comparison

Figures (6 to 14) show that when the pendulum is initially on upper position unstable ($\theta = 0$), it stabilizes after a transitional regime in its desired position due to the V_c control voltage. To confirm the advantages of OFSMC over

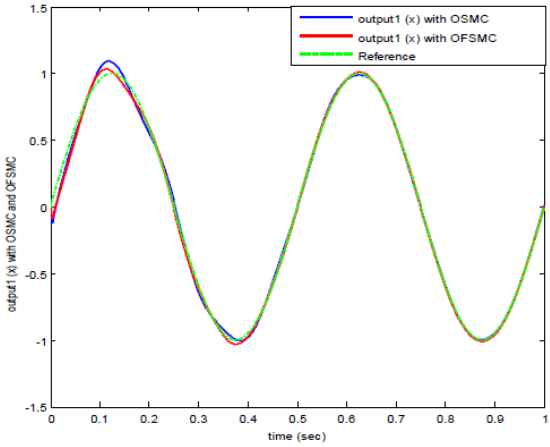

Fig. 5. Output1 (x) with OSMC and OFSMC (1^{st} case).

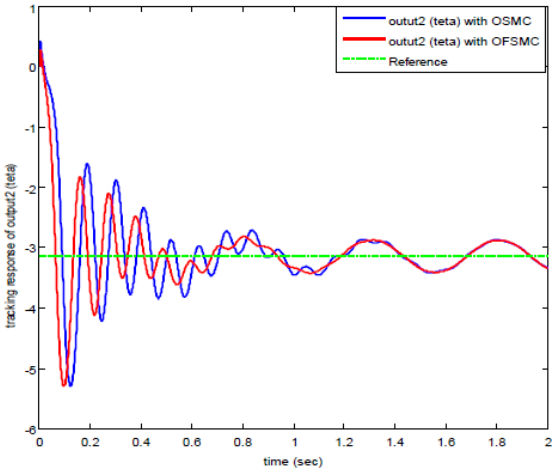

Fig. 6. Output2 (θ) with OSMC and OFSMC (1^{st} case).

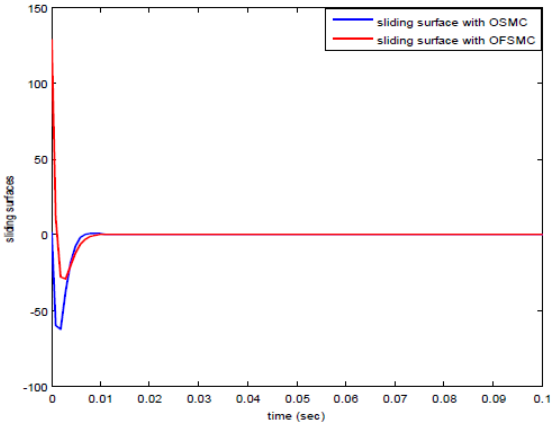

Fig. 7. Zoom of sliding surfaces of OSMC and OFSMC (1^{st} case).

OSMC, the performance of the both controllers is compared in above figures. We adopt the optimal parameters calculated by PSO algorithm, for OSMC and OFSMC controllers. From this simulation results, it can be easily seen that the system state responses with OFSMC is superior to those obtained from applying OSMC controller. Also, comparing the results, the proposed OFSMC possesses not only more accurate control performance but also faster

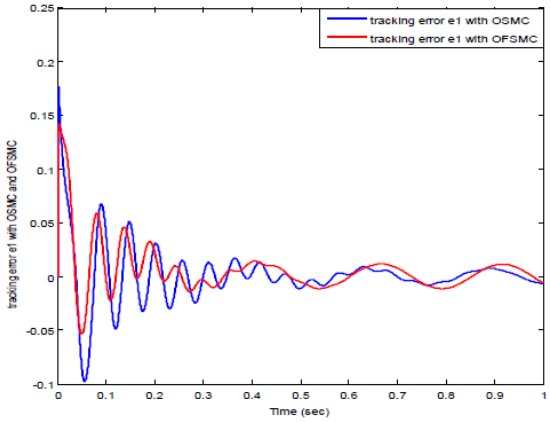

Fig. 8. Tracking error e_1 with OSMC and OFSMC (1^{st} case).

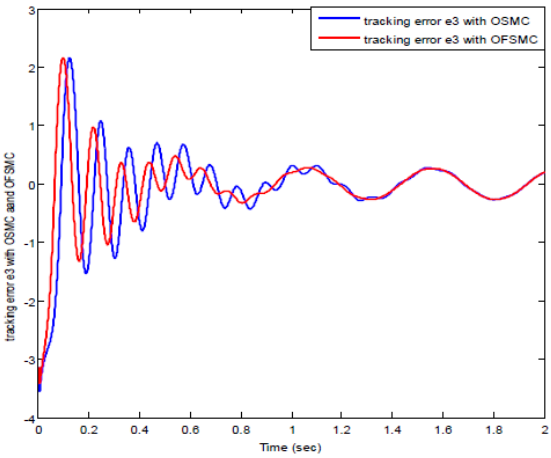

Fig. 9. Zoom of sliding surfaces of OSMC and OFSMC (1^{st} case).

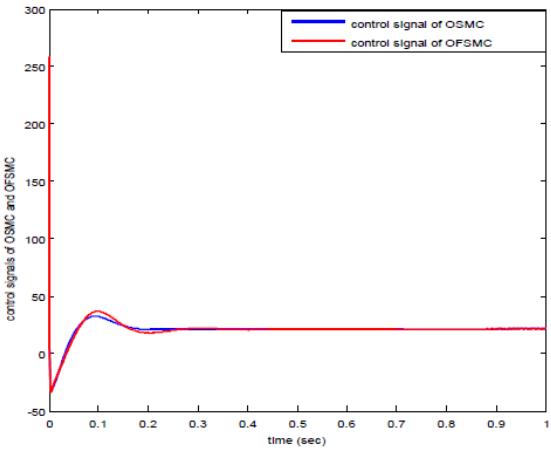

Fig. 10. OSMC and OFSMC Control signals (2^{nd} case).

convergence speed (figures 5, 6, 12 and 13). This study confirms that the proposed OFSMC controller reveals better results and is preferment than OSMC controller.

6. CONCLUSION

[!htbp] In this paper, an optimal fractional-order sliding mode control (OFSMC) and an optimal integer sliding

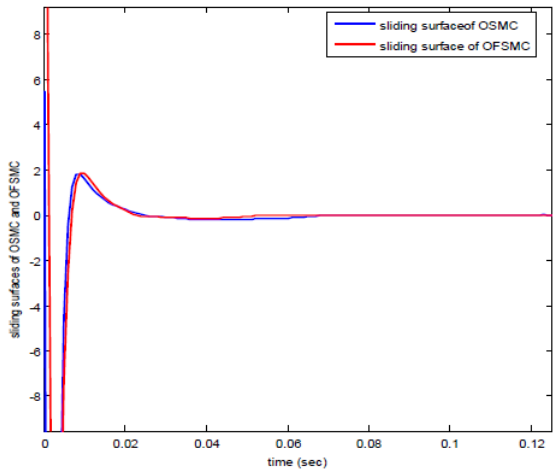

Fig. 11. Zoom of sliding surfaces of OSMC and OFSMC (2^{nd} case).

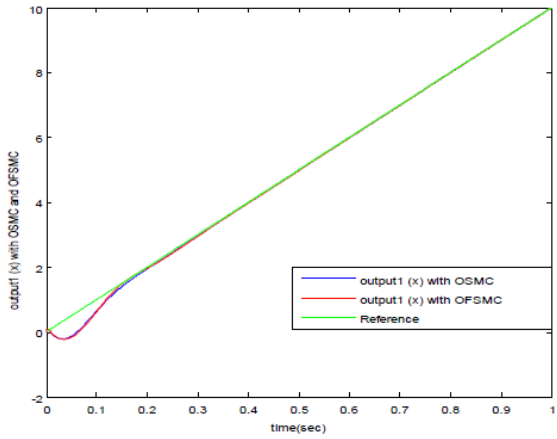

Fig. 12. Output1 (x) with OSMC and OFSMC (2^{nd} case).

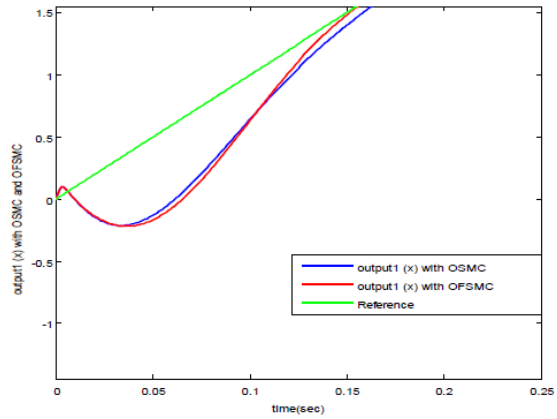

Fig. 13. zoom of Output1 (x) with OSMC and OFSMC (2^{nd} case).

mode control (OSMC) for fractional order nonlinear SIMO systems are investigated. Based on the Lyapunov stability criteria, the OFSMC and OSMC laws control are designed and the tracking of references in closed loop is guaranteed under the proposed controllers. The optimality of proposed approaches are ensured using PSO algorithm. Simulation results have demonstrated the effectiveness and the robustness of the proposed controllers. Besides, the

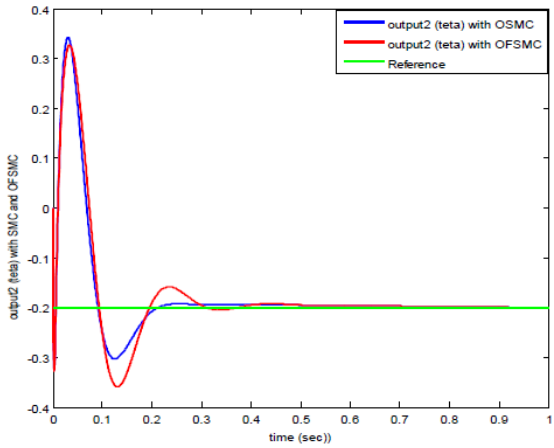

Fig. 14. Output2 (θ) with OSMC and OFSMC ((2^{nd} case).

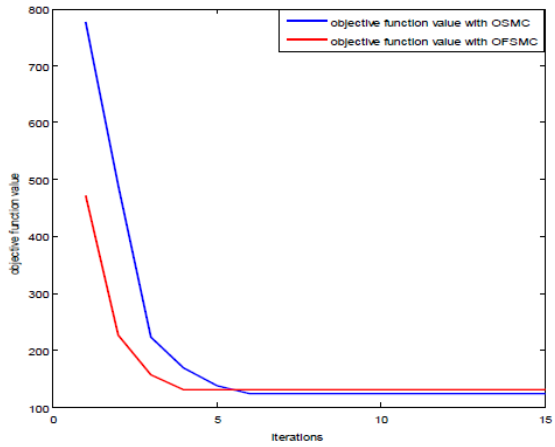

Fig. 15. Objective functions with OSMC and OFSMC (2^{nd} case).

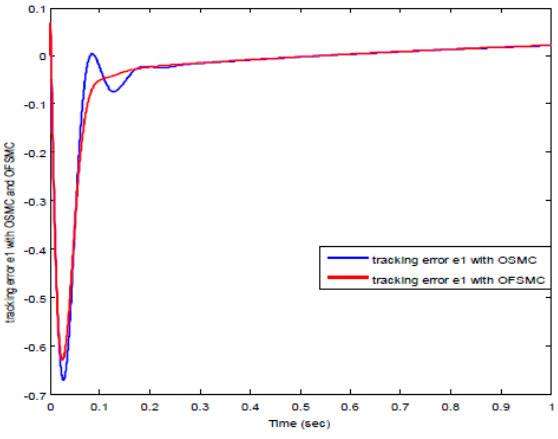

Fig. 16. Tracking error e_1 with OSMC and OFSMC (2^{nd} case).

OFSMC is compared with the OSMC which results in superior performance of the OFSMC. We can also conclude that the choice of a sliding surface should be the same nature with the systems to be controlled, i.e., to design a fractional order sliding mode control for stabilizing this form of fractional order systems, it must select a fractional order sliding surface also contains same derivatives (or integrals) orders of the plants to be stabilized.

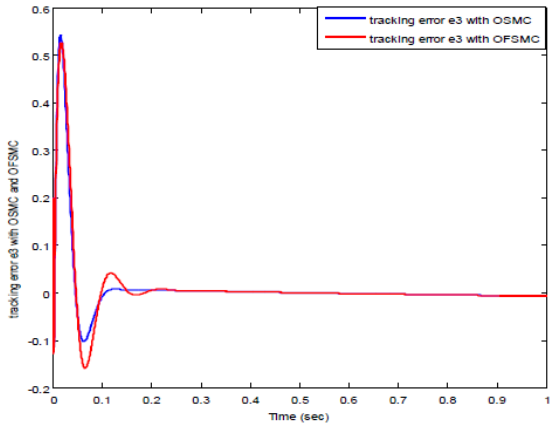

Fig. 17. Tracking error e_3 with OSMC and OFSMC (2^{nd} case).

REFERENCES

Aghababa, M.P. (2012). Robust stabilization and synchronization of a class of fractional-order chaotic systems via a novel fractional sliding mode controller. *Commun Nonlinear Sci Numer-simulat*, vol.17, PP.2670-2681,

Aghababa, M.P. (2013). No-chatter variable structure control for fractional nonlinear complex systems. *journal of Nonlinear Dynamics (NODY)*, vol(73), PP.2329-2342.

Balochian, S., Sedigh, A. K. and Haeri, M. (2011). Stabilization of fractional order systems using a finite number of state feedback laws. *journal of Nonlinear Dynamics (NODY)*, vol.66, PP.141-152.

Calderón A.J., Vinagre B.M. and Feliu V. (2006). Fractional order control strategies for power electronic buck converters. *journal of Signal Processing*, vol.86, n(10) PP.2803-2819.

Chang, W-D. and Shih, S-P. (2010). PID controller design of nonlinear systems using an improved particle swarm optimization approach. *Commun Nonlinear Sci Numer Simulat*, vol.15, PP.3632-3639.

Chiou, J-S. and Liu, M-T. (2009). Numerical simulation for Fuzzy-PID controllers and helping EP Reproduction with PSO hybrid algorithm Simulation. *Modelling Practice and Theory*, vol.17, PP.1555-1565.

Chiu, C-S. (2012). Derivative and integral terminal sliding mode control for a class of MIMO nonlinear systems. *Automatica*, vol.48, pp.316-326.

Clerc, M. (1999). The swarm and the queen: towards a deterministic and adaptive particle swarm optimization. *in- Proceedings of the ICEC 1999, Washington USA*, pp.1951-1957.

Delavari, H., Ranjbar, A.N., Ghaderi, R. and Momani, S. (2010). Fractional order control of a coupled tank. *journal of Nonlinear Dynamics (NODY)*, vol(61), pp.383-397.

Delavari, H., Ghaderi, Ranjbar, R. A. and Momani, S. (2010). Fuzzy fractional order sliding mode controller for nonlinear systems. *Commun Nonlinear Sci Numer Simulat*, vol.15, PP.963-978.

Djari, A., Bouden T. and Boulkroune, A. (2014). Design of Fractional-order Sliding Mode Controller (FSMC) for a class of Fractional-order Non-linear Commensurate

Systems using a Particle Swarm Optimization (PSO) Algorithm. *Journal of control engineering and applied informatics*, CEAI, Vol.16, No.3 pp. 46-55, 2014.

Eberhart, R. C.and Kennedy, J. (1995). A new optimizer using particle swarm theory. *The Sixth International Symposium on Micro Machine and Human Science. Nagoya, Japan*, PP.39-43.

Hosseinnia S. Hassan, Tejado Ines, Vinagre Blas M. and Sierociuk Dominik. (2012) Boolean-based fractional order SMC for switching systems: application to a DC-DC buck converter. *Journal of Signal image and video processing*, vol.6, n3, PP.445-451.

Hosseiia S. Hassan, Tejado I. ,Torres D. and Vinagre B.M. (2014). Vibration suppression controller for a flexible beam on a cart using SMC. *journal of Advances in Intelligent Systems and Computing*, vol.253, PP.127-139.

Ji-Hyuk, Y., Su-Yong, Jung-Hun, S. and Young-Sam, L. (2009). Swing-up Control for an Inverted Pendulum with Restricted Cart Rail Length. *International Journal of Control, Automation, and Systems (IJCASE)*, vol.7(04), pp.674-680.

Kilbas, A. Srivastava, H.M. and Trujillo, J.J. (2006). Theory and Applications of Fractional Differential Equations. *North-Holland Mathematics Studies, Elsevier, Amsterdam, The Netherlands*, vol.204.

Li, C. and Deng, w. (2007). Remarks on fractional derivatives. *Applied Mathematics and Computation*, vol.187, PP.777-784.

Majidabad, S. S., Shandiz, H. T., Hajizadeh,A., and Tohidi, H. (2015). Robust Block Control of Fractional-order Systems via Nonlinear Sliding Mode Techniques. *Journal of control engineering and applied informatics*. CEAI, vol.17, No.1, pp.31-40.

Nour, M., Ooi J. and Chan, K. (2007). Fuzzy Logic Control vs. Conventional PID Control of an Inverted Pendulum. *IEEE Intelligent and Advanced Systems, ICIAS 2007*, PP.209-214.

Oldham, K.B. and Spanier, J. (1974). The Fractional Calculus. *Academic Press, New York, USA*, pp.234.

Oustaloup, A., Mathieu B. and Lanusse, P. (1995). The CRONE control of resonant plants: application to a flexible transmission. *European Journal of Control*, vol.1(02), PP.113-121.

Oustaloup, A., Sabatier, J. and Moreau, X. (1998). From fractal robustness to the CRONE approach. *in Proc. ESAIM: Proceedings*, PP.177-192.

Oustaloup, A., Sabatier J. and Lanusse, P. (1999). From fractal robustness to the CRONE control. *FCAA*, vol.1(02), PP.01-30.

Petras, I. (2011). fractional-order nonlinear systems. *Higher Education Press, Beijing and Springer-Verlag Berlin Heidelberg*, pp.01-18.

Podlubny, I. (1999). Fractional Differential Equations. *Academic Press, New York, USA*, PP.01-119.

Prasad, L., Tyagi B. and Gupta, H. (2012). Modelling and Simulation for Optimal Control of Nonlinear Inverted Pendulum Dynamical System Using PID Controller and LQR. *2012 Sixth IEEE Asia Modelling Symposium*, PP.138-143.

Shi Y. and Eberhart, R.C. (1999). Empirical study of particle swarm optimization. *IEEE*, PP.1945-1950.

Vinagre, B. and Calderon, A. (2006). On fractional sliding mode control. *Proc. Of the 7th Portuguese Conference on Automatic Control, CONTROLO06*. Lisbon, Portugal.

Zhang, B. and Luo, Y. (2012). Fractional order sliding-mode control based on parameters auto-tuning for velocity control of permanent magnet synchronous motor. *ISA Transactions*, vol.51, PP.649-656.